Organometallics **1992,** *11,* 4077–4082

Controlled Double Metalation of Coordinated dppm in Manganese(I) Complexes. The Ligand $[(\mathrm{PPh_2})_2\mathrm{C}]^{2-}$ as a Building Block in the Syntheses of Heterometallic Species

Javier Ruiz, Víctor Riera,* and Marilín Vivanco

Departamento de Química Organometálica, Universidad de Oviedo, 33071 Oviedo, Spain

Santiago García-Granda and Alejandro García-Fernández

Departamento de Química Física y Analítica, Universidad de Oviedo, 33071 Oviedo, Spain

Received June 15, 1992

The cationic complexes *fac*-$[\mathrm{Mn(CNBu^t)(CO)_3(dppm)}]\mathrm{ClO_4}$ (**1a**) and $[\mathrm{Mn(CO)_4(dppm)}]\mathrm{ClO_4}$ (**1b**) are readily deprotonated by KOH in $\mathrm{CH_2Cl_2}$ to give the bis(diphenylphosphino)methanide derivatives *fac*-$[\mathrm{Mn(CNBu^t)(CO)_3\{(Ph_2P)_2CH\}}]$ (**2a**) and $[\mathrm{Mn(CO)_4\{(Ph_2P)_2CH\}}]$ (**2b**). When **2a** and **2b** are reacted with $[\mathrm{Ag(ClO_4)(PPh_3)}]$, the heterodimetallic complexes *fac*-$[\mathrm{Mn(CNBu^t)(CO)_3\{(Ph_2P)_2CH(AgPPh_3)\}}]\mathrm{ClO_4}$ (**3a**) and $[\mathrm{Mn(CO)_4\{(Ph_2P)_2CH(AgPPh_3)\}}]\mathrm{ClO_4}$ (**3b**) are obtained. For **3a** an X-ray analysis has been carried out. Crystal data: monoclinic, space group $P2_1/c$, $a = 11.828$ (3) Å, $b = 24.518$ (5) Å, $c = 17.293$ (6) Å, $\beta = 94.94$ (3)°, $V = 4996$ (2) Å^3, $Z = 4$, $R = 0.033$, $R_w = 0.036$. The heterodimetallic complexes $[\mathrm{Mn(CNBu^t)(CO)_3\{(Ph_2P)_2CH(AuPPh_3)\}}]\mathrm{ClO_4}$ (**4a**) and $[\mathrm{Mn(CO)_4\{(Ph_2P)_2CH(AuPPh_3)\}}]\mathrm{ClO_4}$ (**4b**) have been synthesized by two alternative methods: (a) by treating **1a** and **1b** with 1 equiv of $[\mathrm{AuCl(PPh_3)}]$ and an excess of KOH and (b) by reacting **3a** and **3b** with 1 equiv of $[\mathrm{AuCl(PPh_3)}]$. The treatment of **1a** and **1b** with 2 equiv of $[\mathrm{AuCl(PPh_3)}]$ and an excess of KOH produces the trimetallic species *fac*-$[\mathrm{Mn(CNBu^t)(CO)_3\{(Ph_2P)_2C(AuPPh_3)_2\}}]\mathrm{ClO_4}$ (**5a**) and $[\mathrm{Mn(CO)_4\{(Ph_2P)_2C(AuPPh_3)_2\}}]$ (**5b**), which formally contain the dianion $[(\mathrm{PPh_2})_2\mathrm{C}]^{2-}$. When **4a** is reacted with $[\mathrm{AgCl(PPh_3)}]_4$ in the presence of KOH, the mixed heterotrimetallic species $[\mathrm{Mn(CNBu^t)(CO)_3\{(Ph_2P)_2C(AgPPh_3)(AuPPh_3)\}}]\mathrm{ClO_4}$ (**6a**) is obtained. A mechanism for the formation of **6a** involving the neutral intermediate $[\mathrm{Mn(CNBu^t)(CO)_3\{(Ph_2P)_2C(AuPPh_3)\}}]$ (**7**) is proposed in agreement with the data obtained in the X-ray analysis of **6a**. Crystal data: monoclinic, space group $P2_1/n$, $a = 14.192$ (3) Å, $b = 20.622$ (6) Å, $c = 24.37$ (1) Å, $\beta = 94.91$ (3)°, $V = 7106$ (5) Å^3, $Z = 4$, $R = 0.045$, $R_w = 0.044$.

Introduction

A number of complexes are known to contain bis(diphenylphosphino)methanide ($[(\mathrm{PPh_2})_2\mathrm{CH}]^-$ = dppm-H) as a ligand. In a few cases this ligand acts in a C-bonded monodentate fashion,[1] but in most of the complexes, this group is bidentate (chelate or bridge), bonding to the metal centers by the two phosphorus atoms[1c,d,2] or by a phosphorus and the central carbon atom.[3] The use of $[(\mathrm{PPh_2})_2\mathrm{CH}]^-$ as a tridentate ligand is well established in gold chemistry,[4] though there are also examples in other metals.[5]

Double deprotonation of coordinated bis(diphenylphosphino)methane (dppm) to give complexes formally containing the dianionic ligand $[(\mathrm{PPh_2})_2\mathrm{C}]^{2-}$ has received much less attention in the literature, and as far as we are aware, only three examples are known: $[\mathrm{Pd(\mu\text{-}Cl)_2Pt\{C(PPh_2)_2\}}]_n$,[6] $[\mathrm{(AcOHg)_2\{C(PPh_2)_2\}(HgOAc)_2}]$,[7] and *mer*-$[\mathrm{FeCl(CNPh)_3\{(PPh_2)_2C(AuPPh_3)_2\}}]\mathrm{PF_6}$.[2j] A closely related compound which has the dianion $[\{\mathrm{P(OMe)_2}\}_2\mathrm{C}]^{2-}$ has also been described.[8]

This paper deals with the synthesis of complexes where the ligand $[(\mathrm{PPh_2})_2\mathrm{C}]^{2-}$ is obtained by stepwise controlled deprotonation of coordinated dppm. The synthetic methodology used has revealed itself as an easy way to construct heterometallic species. The preparation of some bidentate and tridentate $[(\mathrm{PPh_2})_2\mathrm{CH}]^-$ derivatives of manganese(I), gold(I), and silver(I) are also described in this paper.

Results and Discussion

Bis(diphenylphosphino)methanide Derivatives. The treatment of dichloromethane solutions of the cationic complexes *fac*-$[\mathrm{Mn(CNBu^t)(CO)_3(dppm)}]\mathrm{ClO_4}$ (**1a**) and $[\mathrm{Mn(CO)_4(dppm)}]\mathrm{ClO_4}$ (**1b**) with an excess of KOH gives, after a few minutes of stirring at room temperature, the neutral bis(diphenylphosphino)methanide derivatives *fac*-$[\mathrm{Mn(CNBu^t)(CO)_3(dppm\text{-}H)}]$ (**2a**) and $[\mathrm{Mn(CO)_4(dppm\text{-}H)}]$ (**2b**), respectively. Complexes **2a** and **2b** are moderately air-stable pale yellow solids. However, in solution exposed to air they slowly decompose to their corresponding protonated species. The preparation of these dppm-H derivatives by using a heterogeneous phase reaction (as KOH is not soluble in $\mathrm{CH_2Cl_2}$) has certain ad-

---

[1] (a) Karsch, H. H.; Appelt, A.; Hanika, G. *J. Organomet. Chem.* **1986**, *312*, C1. (b) Karsch, H. H.; Appelt, A.; Müller, G. *Organometallics* **1986**, *5*, 1664. (c) Balch, A. L.; Oram, D. E. *Organometallics* **1986**, *5*, 2159. (d) Luser, M.; Peringer, P. *J. Organomet. Chem.* **1986**, *312*, C61. (e) Balch, A. L.; Oran, D. E. *Inorg. Chem.* **1987**, *26*, 1906.

[2] (a) Brauer, D. J.; Hietkamp, S.; Stelzer, O. *J. Organomet. Chem.* **1986**, *299*, 137. (b) Brown, M. P.; Yavari, A.; Manojlovic-Muir, L.; Muir, K. W.; Moulding, R. P.; Seddon, K. R. *J. Organomet. Chem.* **1982**, *236*, C33. (c) Schmidbaur, H.; Mandl, J. R. *Angew. Chem., Int. Ed. Engl.* **1977**, *16*, 640. (d) Browning, J.; Bushnell, G. W.; Dixon, K. R. *J. Organomet. Chem.* **1980**, *198*, C11. (e) Briant, C. E.; Hall, K. P.; Mingos, D. M. P. *J. Organomet. Chem.* **1982**, *229*, C5. (f) Al-Jibori, S.; Shaw, B. L. *J. Chem. Soc., Chem. Commun.* **1982**, 286. (g) Issleib, V. K.; Abicht, H. P.; Winkelmann, H. *Z. Anorg. Allg. Chem.* **1972**, *388*, 89. (h) Bassett, J. M.; Mandl, J. R.; Schmidbaur, H. *Chem. Ber.* **1982**, *113*, 1145. (i) Riera, V.; Ruiz, J. *J. Organomet. Chem.* **1986**, *310*, C36. (j) Riera, V.; Ruiz, J.; Solans, X.; Tauler, E. *J. Chem. Soc., Dalton Trans.* **1990**, 1607. (k) Karsch, H. H.; Appelt, A.; Müller, G. *Organometallics* **1986**, *5*, 1664.

[3] (a) Schmidbaur, H.; Lauteschläger, S.; Müller, G. *J. Organomet. Chem.* **1985**, *281*, 33. (b) Brown, M. P.; Yavari, A.; Manojlovic-Muir, Lj.; Muir, K. W. *J. Organomet. Chem.* **1983**, *256*, C19.

[4] Laguna, A.; Laguna, M. *J. Organomet. Chem.* **1990**, *394*, 743 and references therein.

[5] (a) Clucas, J. A.; Harding, M. M.; Nicholls, B. S.; Smith, A. K. *J. Chem. Soc., Dalton Trans.* **1985**, 1835. (b) Dawkins, G. M.; Green, M.; Jeffery, J. C.; Sambale, C.; Stone, F. G. A. *J. Chem. Soc., Dalton Trans.* **1983**, 499. (c) Camus, A.; Marisch, N.; Nardin, G.; Randaccio, L. *J. Organomet. Chem.* **1973**, *60*, C39.

[6] Al-Resayes, S. I.; Hitchcock, P. B.; Nixon, J. F. *J. Chem. Soc., Chem. Commun.* **1986**, 1710.

[7] Lusser, M.; Peringer, P. *Organometallics* **1984**, *3*, 1916.

[8] Payne, N. C.; Ramachandran, R.; Treurnicht, I.; Puddephatt, R. J. *Organometallics* **1990**, *9*, 880.

0276-7333/92/2311-4077$03.00/0

Scheme I

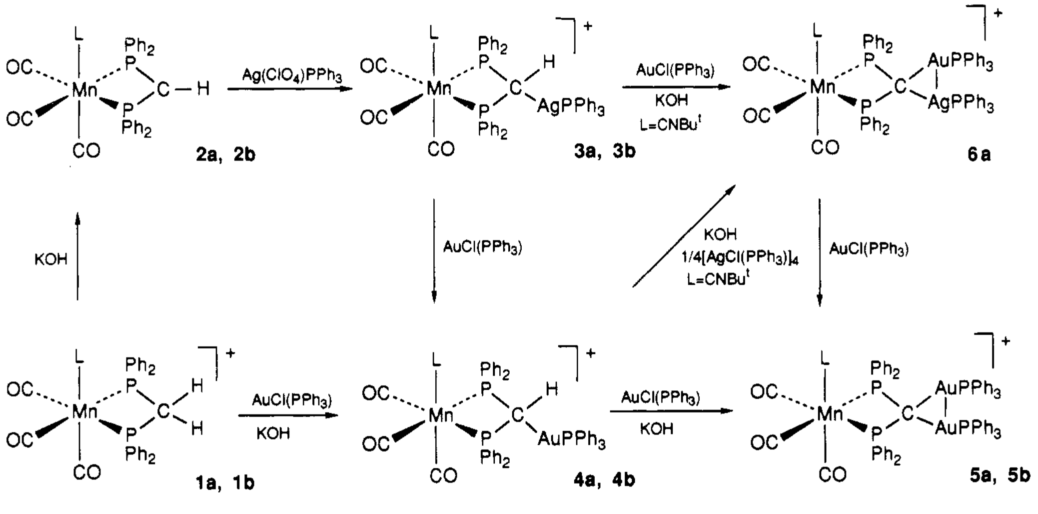

L = CO, CNBu^t

vantages. It allows the easy elimination of the KClO$_4$ and the excess KOH by means of simple filtration. At the same time the H$_2$O formed is retained by the excess of KOH used. Finally, the reaction rate is slow enough to be controlled by IR spectroscopy.

As expected, a change toward low frequencies for the ν(CO) and ν(CN) bands was observed in the infrared spectra of **2a** and **2b** when compared with those of their cationic precursors (see Table I). Naturally this effect corresponds to an increased back-bonding between the metal and the CO and CNBu^t groups in the electronically richer neutral complexes.

The ^{1}H NMR spectra of **2a** and **2b** have, as the most characteristic signal, a triplet about 2.4 ppm assignable to the proton of the central carbon atom in the methanide ligand. The ^{31}P{^{1}H} NMR spectra of these complexes present a broad singlet for the two equivalent phosphorus atoms but at a lower frequency than for the starting compounds **1a** and **1b** (Table I). The broadening of the phosphorus signals is due to the quadrupolar moment effect of manganese (^{55}Mn, $I = {}^5/_2$). This is general for all of the manganese-bonded phosphorus signals appearing in this paper, so henceforth we will not make any further comment on the matter.

Heterodimetallic Species. The complexes **2a** and **2b** are suitable starting materials for the syntheses of heterometallic species because they contain a potentially tridentate dppm-H ligand. In fact, when these complexes are treated with 1 equiv of [Ag(ClO$_4$)(PPh$_3$)], the compounds *fac*-[Mn(CNBu^t)(CO)$_3${(PPh$_2$)$_2$CH(AgPPh$_3$)}]ClO$_4$ (**3a**) and [Mn(CO)$_4${(PPh$_2$)$_2$CH(AgPPh$_3$)}]ClO$_4$ (**3b**) are readily obtained (see Scheme I). The IR spectra of **3a** and **3b** in the ν(CO) region show a pattern of bands similar to that for the dppm derivatives *fac*-[Mn(CNBu^t)(CO)$_3$(dppm)]ClO$_4$ (**1a**) and [Mn(CO)$_4$(dppm)]ClO$_4$ (**1b**) but at lower frequencies, thus showing that the fragment [Ag(PPh$_3$)]$^+$ is less able to neutralize the excess of electronic density on the central carbon atom of the methanide ligand than the proton.

In the ^{31}P{^{1}H} NMR spectrum of **3a** the resonance due to PPh$_3$ appears as a pair of doublets due to splitting by ^{107}Ag ($I = {}^1/_2$; natural abundance 51.82%; ^1J(AgP) = 512.5 Hz) and ^{109}Ag ($I = {}^1/_2$; natural abundance 48.18%; ^1J(AgP) = 591.7 Hz), and each component is further split into a triplet by coupling to the two equivalent phosphorus atoms of the diphosphine (^3J(PP) = 5.8 Hz). A similar pattern of signals is observed in the ^{31}P{^{1}H} NMR spectrum of **3b**, although not as good a resolution as for **3a** was found.

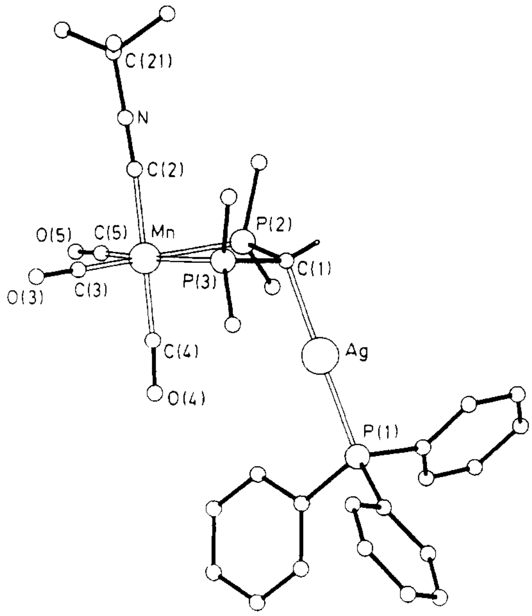

Figure 1. PLUTO drawing of the structure of the cation of *fac*-[Mn(CNBu^t)(CO)$_3${(PPh$_2$)$_2$CH(AgPPh$_3$)}]ClO$_4$ (**3a**) with numbering scheme. The phenyl groups of the diphosphine are omitted for clarity.

The structure of the compound *fac*-[Mn(CNBu^t)(CO)$_3${(PPh$_2$)$_2$CH(AgPPh$_3$)}]ClO$_4$ (**3a**) was determined by X-ray crystallography, and a view of the complex cation is shown in Figure 1. Manganese is pseudooctahedrally coordinated by three carbonyl groups in a facial arrangement, the two phosphorus atoms of the diphosphine, and the *tert*-butyl isocyanide ligand. Silver has an almost linear coordination geometry, being bonded to the central carbon atom of the diphosphine and to the triphenylphosphine ligand. The fragment [Ag(PPh$_3$)] is located anti with respect to the isocyanide ligand, and this probably implies that the attack of [Ag(ClO$_4$)(PPh$_3$)] on the methanide was trans to the bulky *tert*-butyl isocyanide group.

The distances P(2)–C(1) (1.784 (4) Å) and P(3)–C(1) (1.784 (4) Å) are intermediate between those in dppm complexes[9] (1.84 Å) and those in dppm-H derivatives[1,2] (1.72–1.74 Å). This suggests that a multiple-bond character

---

[9] Puddephatt, R. J. *Chem. Soc. Rev.* **1983**, *12*, 99.

Table I. IR[a] and NMR[b] Data for the Complexes

compd	*ν*(CO), cm^{-1}	*ν*(CN), cm^{-1}	^{1}H NMR, *δ* (*J*, Hz)[c]	^{31}P{^{1}H} NMR, *δ* (*J*, Hz)[d]
1a	2040 s 1979 s	2180 m	0.74 (s, Bu^t) 5.25 (m, *AB*X$_2$, H$_A$ 5.16, H$_B$ 5.35, *J*(HH) = 17, *J*(HP) = 11)	11 (br)
1b	2094 m 2027 m 2014 s 1999 sh		5.23 (t, *J*(PH) = 11)[e]	7.5 (br)[e]
2a	2011 vs 1946 s 1925 s	2171 m	0.56 (s, Bu^t)[f] 2.41 (t, P$_2$C–H, *J*(PH) = 4.8)	–3.3 (br)
2b	2071 m 1990 s 1955 m		2.36 (t, P$_2$C–H, *J*(PH) = 4.4)[f]	–9.1 (br)
3a	2027 s 1956 s	2181 m	0.62 (s, Bu^t)[e] 5.10 (m, P$_2$C–H)	18.5 (br, P–Mn)[f] 14.1 (dt, P–^{109}Ag, ^1J(^{109}AgP) = 592, ^3J(PP) = 5.8) 14.1 (dt, P–^{107}Ag, ^1J(^{107}AgP) = 512, ^3J(PP) = 5.8)
3b	2082 m 2013 m 1993 s 1976 sh		5.67 (m, P$_2$C–H)	12.1 (br, P–Mn) 14.2 (d, P–^{109}Ag, ^1J(^{109}AgP) = 611) 14.2 (d, P–^{107}Ag, ^1J(^{107}AgP) = 529)
4a	2031 s 1963 s	2181 m	0.63 (s, Bu^t) 5.70 (sq, P$_2$C–H, ^2J(PH) = 10, ^3J(PH) = 10)	23.1 (br, P–Mn) 39.3 (t, P–Au, ^3J(PP) = 9.5)
4b	2086 m 2020 m 2001 s 1988 sh		5.95 (sq, P$_2$C–H, ^2J(PH) = 10, ^3J(PH) = 10)	16.5 (br, P–Mn) 38.9 (t, P–Au, ^3J(PP) = 12)
5a	2022 vs 1952 s	2176 m	0.64 (s, Bu^t)	33.66 (br, P–Mn) 35.07 (td, P–Au, ^3J(P$_{\mathrm{Mn}}$P$_{\mathrm{Au}}$) = 10.6, ^3J(P$_{\mathrm{Au}}$P$_{\mathrm{Au}}$) = 4) 38.26 (td, P–Au, ^3J(P$_{\mathrm{Mn}}$P$_{\mathrm{Au}}$) = 7.2, ^3J(P$_{\mathrm{Au}}$P$_{\mathrm{Au}}$) = 4)
5b	2078 s 2010 s 1993 vs 1977 s			26.1 (s, br, P–Mn) 35.8 (t, P–Au, ^3J(PP) = 8.1)
6a	2019 s 1947 s	2176 m	0.57 (s, Bu^t)	29.43 (br, P–Mn) 10.81 (dt, P–Ag, ^1J(^{109}AgP) = 564, ^3J(P$_{\mathrm{Mn}}$P$_{\mathrm{Ag}}$) = 6) 10.81 (dt, P–Ag, ^1J(^{107}AgP) = 490, ^3J(P$_{\mathrm{Mn}}$P$_{\mathrm{Ag}}$) = 6) 42.06 (t, P–Au, ^3J(P$_{\mathrm{Mn}}$P$_{\mathrm{Au}}$) = 6)

[a] In Cl$_2$CH$_2$ solutions. Abbreviations: vs, very strong; s, strong; m, medium; sh, shoulder. [b] In CDCl$_3$ solutions. Abbreviations: s, singlet; d, doublet; t, triplet; sq, pseudoquartet; dt, doublet of triplets; td, triple of doublets; m, multiplet; br, broad. [c] *δ* from internal TMS. Resonances for phenyl hydrogens are not given. [d] In CDCl$_3$ solutions, *δ* from external 85% H$_3$PO$_4$. [e] In Cl$_2$CD$_2$ solutions. [f] At –40 °C.

Table II. Selected Fractional Positional and Thermal Parameters (with Esd's) for $[\mathrm{Mn(CNBu^t)(CO)_3\{(Ph_2P)_2CH(AgPPh_3)\}]ClO_4}$ (3a)

atom	*x*	*y*	*z*	100*U*$_{\mathrm{eq}}$,[a] Å^2
Ag	0.27876 (3)	0.66486 (1)	0.27531 (2)	5.19 (1)
Mn	0.31154 (5)	0.49439 (2)	0.33725 (3)	4.83 (2)
P(1)	0.38404 (8)	0.74635 (4)	0.30404 (6)	4.70 (3)
P(2)	0.31484 (8)	0.54085 (4)	0.21914 (5)	4.38 (3)
P(3)	0.15367 (9)	0.55220 (4)	0.31828 (5)	4.51 (3)
C(1)	0.2026 (3)	0.5866 (1)	0.2366 (2)	4.1 (1)
C(3)	0.2805 (4)	0.4644 (2)	0.4292 (3)	7.2 (2)
O(3)	0.2609 (4)	0.4452 (2)	0.4868 (2)	12.0 (2)
C(4)	0.3894 (4)	0.5489 (2)	0.3879 (2)	6.4 (2)
O(4)	0.4405 (3)	0.5816 (1)	0.4232 (2)	9.9 (2)
C(5)	0.4416 (4)	0.4568 (2)	0.3286 (3)	6.7 (2)
O(5)	0.5271 (3)	0.4352 (1)	0.3221 (3)	10.8 (2)
C(2)	0.2228 (4)	0.4357 (2)	0.2859 (2)	5.2 (1)
N	0.1708 (3)	0.3998 (1)	0.2595 (2)	6.1 (1)
C(21)	0.1005 (4)	0.3537 (2)	0.2280 (3)	6.7 (2)

[a] $U_{\mathrm{eq}} = {}^1/_3\sum_i\sum_j U_{ij}a_ia_j\mathbf{a}_i{}^*\mathbf{a}_j{}^*$.

Table III. Selected Bond Lengths (Å) and Bond Angles (deg) (with Esd's) for $[\mathrm{Mn(CNBu^t)(CO)_3\{(Ph_2P)_2CH(AgPPh_3)\}]ClO_4}$ (3a)

Ag–P(1)	2.384 (1)	Ag–C(1)	2.200 (4)	Mn–P(2)	2.342 (1)
Mn–P(3)	2.345 (1)	Mn–C(3)	1.817 (5)	Mn–C(4)	1.806 (5)
Mn–C(5)	1.810 (5)	Mn–C(2)	1.950 (4)	P(2)–C(1)	1.783 (4)
P(3)–C(1)	1.784 (4)	C(3)–O(3)	1.144 (5)	C(4)–O(4)	1.148 (5)
C(5)–O(5)	1.156 (5)	C(2)–N	1.145 (5)	N–C(21)	1.479 (5)

C(1)–Ag–P(1)	170.9 (1)	P(3)–Mn–P(2)	69.9 (1)
C(3)–Mn–P(2)	168.3 (2)	C(3)–Mn–P(3)	98.5 (1)
C(4)–Mn–P(2)	91.0 (1)	C(4)–Mn–P(3)	89.3 (1)
C(4)–Mn–C(3)	90.4 (2)	C(5)–Mn–P(2)	95.6 (1)
C(5)–Mn–P(3)	165.5 (1)	C(5)–Mn–C(3)	95.9 (2)
C(5)–Mn–C(4)	90.8 (2)	C(2)–Mn–P(2)	90.6 (1)
C(2)–Mn–P(3)	89.5 (1)	C(2)–Mn–C(3)	87.6 (2)
C(2)–Mn–C(4)	177.5 (2)	C(2)–Mn–C(5)	90.8 (2)
C(1)–P(2)–Mn	95.1 (1)	C(1)–P(3)–Mn	95.0 (1)
P(2)–C(1)–Ag	108.0 (2)	P(3)–C(1)–Ag	108.9 (2)
P(3)–C(1)–P(2)	97.7 (2)	O(3)–C(3)–Mn	179.4 (4)
O(4)–C(4)–Mn	176.4 (4)	O(5)–C(5)–Mn	176.7 (4)
N–C(2)–Mn	176.3 (4)	C(21)–N–C(2)	177.7 (4)

remains between the phosphorus and the carbon atoms, although it is not as noticeable as in the starting methanide complexes. The CNC angle in the *tert*-butyl isocyanide ligand is almost linear (177.7 (4)°). This is normal for a rather electronically poor metal center, such as manganese(I), coordinated by three strongly electron-withdrawing carbonyl ligands. Other bond lengths and angles for **3a** are summarized in Table III.

The heterodimetallic manganese–gold complexes *fac*-$[\mathrm{Mn(CNBu^t)(CO)_3\{(PPh_2)_2CH(AuPPh_3)\}]ClO_4}$ (**4a**) and $[\mathrm{Mn(CO)_4\{(PPh_2)_2CH(AuPPh_3)\}]ClO_4}$ (**4b**), which are structurally analogous to **3a** and **3b**, have been obtained in two different ways (see scheme I): (a) by treating **1a** and **1b** with 1 equiv of [AuCl(PPh$_3$)] in the presence of an excess of KOH in dichloromethane and (b) by reacting **3a** and **3b** with 1 equiv of [AuCl(PPh$_3$)] in dichloromethane. Naturally, with this last method, the formation of [AgCl(PPh$_3$)]$_4$ occurs. The greater strength of the Ag–Cl bond compared to that of the Au–Cl bond could be the driving force for this last reaction.

Scheme II

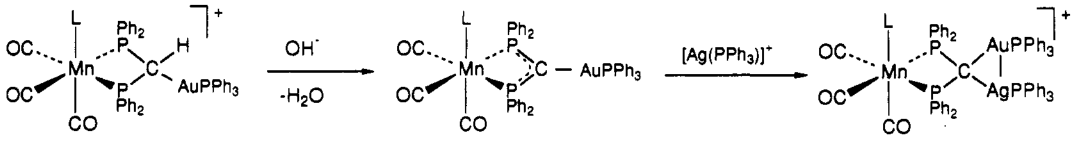

4a **7** **6a**

L = $CNBu^t$

The preparation of **4b** is best achieved by following method b, because if method a is used, it is difficult to avoid the formation of some amounts of $[Mn(CO)_4\{(PPh_2)_2C(AuPPh_3)_2\}]ClO_4$ (**5b**), whose rational synthesis will be described later.

The $^{31}P\{^1H\}$ NMR spectra of **4a** and **4b** show a triplet for the PPh_3 phosphorus and a broad signal for the two phosphorus atoms of the diphosphine. In their ^1H NMR spectra the P_2C–H proton appears as a pseudoquartet, probably due to a similar value of $^2J(PH)$ and $^3J(PH)$ (Table I).

Heterotrimetallic Species. Double deprotonation of coordinated dppm in **1a** and **1b** has been achieved by heterogeneous phase basic treatment of these complexes in the presence of the appropriate metallic fragments, yielding in this way trimetallic species. Thus, when **1a** and **1b** are treated with 2 equiv of $[AuCl(PPh_3)]$ in the presence of an excess of KOH in dichloromethane, the complexes *fac*-$[Mn(CNBu^t)(CO)_3\{(PPh_2)_2C(AuPPh_3)_2\}]ClO_4$ (**5a**) and $[Mn(CO)_4\{(PPh_2)_2C(AuPPh_3)_2\}]ClO_4$ (**5b**) are readily obtained. Monitoring the reaction by IR spectroscopy in the $\nu(CO)$ and $\nu(CN)$ region shows, in the first step, the formation of **4a** and **4b**, which completely disappear to give **5a** and **5b** as the reaction progresses.

The $^{31}P\{^1H\}$ NMR spectrum of **5a** gives two triplets of doublets for the two inequivalent PPh_3 groups: the one that is located syn with respect to the $CNBu^t$ ligand and the one that is located anti with respect to this group. In the case of **5b** the two PPh_3 groups are obviously equivalent and only one triplet can be observed.

The synthetic method used for the preparation of the trimetallic species allows the coordination of two different metallic fragments to the central carbon atom of the diphosphine, as exemplified by the mixed complex *fac*-$[Mn(CNBu^t)(CO)_3\{(PPh_2)_2C(AuPPh_3)(AgPPh_3)\}]ClO_4$ (**6a**) obtained by treating *fac*-$[Mn(CNBu^t)(CO)_3\{(PPh_2)_2CH(AuPPh_3)\}]ClO_4$ (**4a**) with $[AgCl(PPh_3)]_4$ in the presence of an excess of KOH (see Scheme I).

In the $^{31}P\{^1H\}$ NMR spectrum of **6a**, the phosphorus of the fragment $[Au(PPh_3)]$ gives a triplet, which results from coupling to the two phosphorus atoms of the diphosphine. The resonance of the phosphorus in the $[Ag(PPh_3)]$ group is a pair of doublets of triplets owing to splitting by ^{107}Ag, ^{109}Ag, and the two phosphorus nuclei of the diphosphine.

Complex **6a** can also be obtained directly by treating a dichloromethane solution of *fac*-$[Mn(CNBu^t)(CO)_3\{(PPh_2)_2CH(AgPPh_3)\}]ClO_4$ (**3a**) with 1 equiv of $[AuCl(PPh_3)]$ and an excess of KOH. Monitoring the reaction by IR spectroscopy shows in the first step the formation of *fac*-$[Mn(CNBu^t)(CO)_3\{(PPh_2)_2CH(AuPPh_3)\}]ClO_4$ (**4a**). At the same time, the compound $[AgCl(PPh_3)]_4$ must be generated as a result. Finally, these two species, in the presence of KOH, yield **6a**. Following a behavior similar to that observed for **3a**, the fragment $[Ag(PPh_3)]$ in **6a** can be easily replaced by the fragment $[Au(PPh_3)]$ to give **5a** by treatment with 1 equiv of $[AuCl(PPh_3)]$ (see Scheme I).

Table IV. Selected Fractional Positional and Thermal Parameters (with Esd's) for $[Mn(CNBu^t)(CO)_3\{(Ph_2P)_2(Ag^\dagger PPh_3)(AuPPh_3)\}]ClO_4$ (6a†)

atom	x	y	z	$100U_{eq}$,[a] Å^2
Au	0.14740 (4)	0.04671 (3)	0.23327 (2)	4.42 (2)
Ag†	0.34186 (6)	0.02603 (4)	0.21106 (3)	4.77 (4)
Mn	0.4156 (2)	0.0276 (1)	0.3864 (1)	6.0 (1)
P(1)	0.0195 (3)	0.0666 (2)	0.1726 (2)	4.8 (2)
P(2)	0.4046 (3)	0.0117 (2)	0.1274 (2)	5.1 (2)
P(3)	0.3056 (3)	−0.0318 (2)	0.3296 (2)	4.6 (2)
P(4)	0.3197 (3)	0.0961 (2)	0.3295 (2)	4.9 (2)
C(1)	0.2664 (8)	0.0340 (6)	0.2860 (5)	3.7 (5)
C(3)	0.482 (2)	0.089 (1)	0.4251 (7)	10 (1)
O(3)	0.521 (1)	0.1306 (9)	0.4485 (6)	15.2 (9)
C(4)	0.473 (1)	−0.037 (1)	0.4214 (7)	8.8 (9)
O(4)	0.513 (1)	−0.0823 (8)	0.4435 (6)	11.8 (8)
C(5)	0.500 (1)	0.0230 (9)	0.3339 (8)	7.4 (8)
O(5)	0.5529 (8)	0.0169 (7)	0.3007 (5)	9.6 (6)
C(2)	0.328 (1)	0.0321 (8)	0.4411 (7)	6.1 (7)
N	0.2796 (9)	0.0355 (7)	0.4772 (5)	6.7 (6)
C(21)	0.220 (1)	0.041 (1)	0.5225 (7)	7.6 (8)

[a] $U_{eq} = {}^1/_3\sum_i\sum_j U_{ij}a_ia_j\mathbf{a}_i^*\mathbf{a}_j^*$.

A likely reaction pathway for the formation of **6a** is shown in Scheme II. Deprotonation of **4a** with KOH gives the proposed neutral intermediate **7**, which is closely related to the methanide derivative **2a** on the basis of the isolobal connection H↔$AuPPh_3$. Intermediate **7** should be a very reactive species, as it has an excess of electronic density on the central carbon atom of the diphosphine, and could give a nucleophilic attack on $[AgCl(PPh_3)]_4$ (the source of the $[Ag(PPh_3)]^+$ fragment) to yield **6a**. It is very probable that, due to steric reasons, this attack occurs anti with respect to the bulky $CNBu^t$ group; so in the final product the fragment $[Au(PPh_3)]$ should be located syn to the $CNBu^t$ group, thus changing its original position in the starting material **4a**.

With the analytical and spectroscopic data we have for **6a**, it is not possible to distinguish between the two isomers that arise from the two relative positions of the $[Au(PPh_3)]$ and $[Ag(PPh_3)]$ fragments. For this reason, and in order to support structurally the mechanism proposed in Scheme II, an X-ray analysis for **6a** has been undertaken. Unfortunately, during the slow process of crystallization used to obtain suitable single crystals, some decomposition occurred, resulting in the formation of a mixture of **6a** and **5a** in an approximate 2:1 ratio, respectively (by $^{31}P\{^1H\}$ NMR of the crystals). This ratio is approximately the same in the monocrystal chosen for the X-ray analysis, as can be deduced from the occupancy refinement made (see the X-ray analysis considerations in the Experimental Section). In this context, the crystallographic data shown in Tables IV and V should be regarded as average values for the two independent cations present in the monocrystal. Note that the only difference between these two cations is the presence of the fragment $[Au(PPh_3)]$ in **5a**, whereas there is the fragment $[Ag(PPh_3)]$ in **6a**. The structure of this mixture of cations (that has been called **6a**†) is represented in Figure 2. Here Ag† refers to the 0.60

Table V. Selected Bond Lengths (Å) and Bond Angles (deg) (with Esd's) for $[Mn(CNBu^t)(CO)_3\{(Ph_2P)_2(Ag^\dagger PPh_3)(AuPPh_3)\}]ClO_4$ (6a†)

Au–Ag†	2.889 (1)	Au–P(1)	2.277 (4)	Au–C(1)	2.05 (1)
Ag†–P(2)	2.313 (4)	Ag†–C(1)	2.20 (1)	Mn–P(3)	2.342 (5)
Mn–P(4)	2.333 (5)	Mn–C(3)	1.80 (2)	Mn–C(4)	1.75 (2)
Mn–C(5)	1.82 (2)	Mn–C(2)	1.91 (2)	P(3)–C(1)	1.78 (1)
P(4)–C(1)	1.79 (1)	C(3)–O(3)	1.14 (2)	C(4)–O(4)	1.20 (2)
C(5)–O(5)	1.16 (2)	C(2)–N	1.16 (2)	N–C(21)	1.46 (2)

P(1)–Au–Ag†	128.7 (1)	C(1)–Au–Ag†	49.4 (3)
C(1)–Au–P(1)	176.4 (4)	P(2)–Ag†–Au	129.1 (1)
C(1)–Ag†–Au	45.0 (3)	C(1)–Ag†–P(2)	173.0 (3)
P(4)–Mn–P(3)	68.9 (2)	C(3)–Mn–P(3)	166.5 (8)
C(3)–Mn–P(4)	97.9 (7)	C(4)–Mn–P(3)	98.6 (7)
C(4)–Mn–P(4)	167.6 (7)	C(4)–Mn–C(3)	95 (1)
C(5)–Mn–P(3)	90.1 (5)	C(5)–Mn–P(4)	89.9 (6)
C(5)–Mn–C(3)	93.3 (8)	C(5)–Mn–C(4)	89.8 (8)
C(2)–Mn–P(3)	89.7 (5)	C(2)–Mn–P(4)	90.2 (5)
C(2)–Mn–C(3)	86.8 (8)	C(2)–Mn–C(4)	90.1 (8)
C(2)–Mn–C(5)	179.8 (3)	Ag†–C(1)–Au	85.6 (4)
P(3)–C(1)–Au	132.0 (7)	P(3)–C(1)–Ag†	106.7 (6)
P(4)–C(1)–Ag†	109.5 (6)	C(1)–P(3)–Mn	96.4 (5)
C(1)–P(4)–Mn	96.6 (4)	P(4)–C(1)–Au	124.3 (7)
P(4)–C(1)–P(3)	95.6 (6)	O(3)–C(3)–Mn	176 (2)
O(4)–C(4)–Mn	177 (2)	O(5)–C(5)–Mn	177 (2)
N–C(2)–Mn	175 (2)	C(21)–N–C(2)	179 (2)

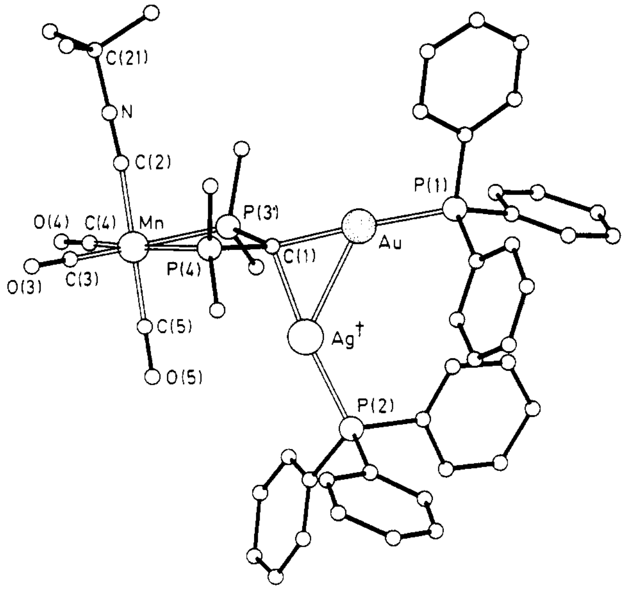

Figure 2. PLUTO drawing of the structure of the cation of *fac*-$[Mn(CNBu^t)(CO)_3\{(PPh_2)_2C(Ag^\dagger PPh_3)(AuPPh_3)\}]ClO_4$ (**6a**†) with numbering scheme. The phenyl groups of the diphosphine are omitted for clarity.

Ag/0.40 Au mixture in this position. The most important feature, for our purposes, in the structure is the situation of the fragment $[Ag(PPh_3)]$, which is located anti with respect to the $CNBu^t$ ligand, and this is in agreement with the mechanism proposed in Scheme II for the formation of **6a**. The great similarity existing between silver(I) and gold(I) is made evident by the fact that no high standard deviation is found in the position of the Ag† and P(2) atoms. The Ag†–Au distance of 2.891 (1) Å is in the range expected for Ag–Au clusters,[10] which, on the other hand, is the same as that found in Au–Au clusters.[10] This clearly means that there is a bonding interaction between the silver and gold atoms in **6a** and between the two gold atoms in **5a**. The distances between the phosphorus atoms and the central carbon atom in the diphosphine (P(3)–C(1) = 1.78 (1) Å, P(4)–C(1) = 1.79 (1) Å) are slightly shorter than those usually found in dppm derivatives,[9] indicating once again that a multiple-bond character exists, although not as noticeable as in the methanide derivatives.

In conclusion, we feel that the synthetic route followed for the preparation of the heterotrimetallic species with the ligand $[(PPh_2)_2C]^{2-}$ described in this paper may be general, affording a new way to obtain a number of heterometallic species by adequately choosing the different metallic fragments.

Experimental Section

General Remarks. All reactions were performed under a nitrogen atmosphere by using standard Schlenk techniques. Solvents were dried and purified by standard techniques and distilled under nitrogen prior to use. CH_2Cl_2 and $CDCl_3$ were treated with anhydrous Na_2CO_3 and stored under nitrogen.

The compounds $[Mn(CO)_4(dppm)]ClO_4$[11] (**1b**), *fac*-$[Mn(CNBu^t)(CO)_3(dppm)]ClO_4$[12] (**1a**), $[AuCl(PPh_3)]$,[13] $[AgCl(PPh_3)]_4$,[14] and $[Ag(ClO_4)(PPh_3)]$[15] were prepared according to literature procedures. All other reagents were used as obtained from commercial sources.

Infrared spectra were recorded on a Perkin-Elmer FT1720-X spectrophotometer. Proton and phosphorus magnetic resonance spectra (NMR) were recorded on a Bruker AC-300 spectrometer. Chemical shifts are referenced to internal TMS (^1H) or external 85% H_3PO_4 (^{31}P). Elemental analyses were carried out on a Perkin-Elmer 240-B microanalyzer.

***fac*-$[Mn(CNBu^t)(CO)_3\{(Ph_2P)_2CH\}]$ (2a).** To a stirred solution of *fac*-$[Mn(CNBu^t)(CO)_3(dppm)]ClO_4$ (**1a**; 0.50 g, 0.71 mmol) in 50 mL of CH_2Cl_2 at room temperature, an excess of KOH (1.0 g, 18 mmol) was added. The mixture was stirred for 30 min, after which the solvent was removed under reduced pressure. The residue was extracted with toluene (50 mL) and filtered off; the extract was concentrated under reduced pressure, and the product **2a** was obtained as yellow crystals (0.39 g, 91% yield). Anal. Calcd for $C_{33}H_{30}MnNO_3P_2$: C, 65.46; H, 4.99; N, 2.31. Found: C, 65.57; H, 4.98; N, 2.19.

The corresponding complex $[Mn(CO)_4\{(Ph_2P)_2CH\}]$ (**2b**) was similarly prepared from a solution of $[Mn(CO)_4(dppm)]ClO_4$ (**1b**; 0.40 g, 0.61 mmol) in CH_2Cl_2 (50 mL) and KOH (1.0 g, 18 mmol). The yield was 0.29 g of yellow crystals (87%). Anal. Calcd for $C_{29}H_{21}MnO_4P_2$: C, 63.28; H, 3.85. Found: C, 63.43; H, 3.90.

***fac*-$[Mn(CNBu^t)(CO)_3\{(Ph_2P)_2CH(AgPPh_3)\}]ClO_4$ (3a).** A stoichiometric amount of $[Ag(ClO_4)(PPh_3)]$ (0.155 g, 0.33 mmol) was added to a solution of *fac*-$[Mn(CNBu^t)(CO)_3\{(Ph_2P)_2CH\}]$ (**2a**; 0.20 g, 0.33 mmol) in CH_2Cl_2 (30 mL). The mixture was stirred at room temperature for 15 min. A 15-mL volume of hexane was added, after filtration to remove a violet sediment. The colorless solution was then evaporated to dryness under reduced pressure to give a pale yellow solid. This was recrystallized from CH_2Cl_2/Et_2O, and 0.29 g of pale yellow crystals were obtained (82% yield). Anal. Calcd for $C_{51}H_{45}AgClMnNO_7P_3$: C, 56.98; H, 4.22; N, 1.30. Found: C, 56.87; H, 4.23; N, 1.23.

The same procedure was used for the preparation of $[Mn(CO)_4\{(Ph_2P)_2CH(AgPPh_3)\}]ClO_4$ (**3b**) with 0.20 g (0.36 mmol) of $[Mn(CO)_4\{(Ph_2P)_2CH\}]$ (**2b**) and 0.17 g (0.36 mmol) of $[Ag(ClO_4)(PPh_3)]$: yield 0.29 g, 78%. Anal. Calcd for $C_{47}H_{36}AgClMnO_8P_3$: C, 53.58; H, 3.56. Found: C, 53.60; H, 3.60.

***fac*-$[Mn(CNBu^t)(CO)_3\{(Ph_2P)_2CH(AuPPh_3)\}]ClO_4$ (4a). Method a.** A solution of *fac*-$[Mn(CNBu^t)(CO)_3(dppm)]ClO_4$ (**1a**; 0.20 g, 0.28 mmol) in CH_2Cl_2 (40 mL) was treated with KOH (0.3 g, 5.3 mmol) and $[AuCl(PPh_3)]$ (0.14 g, 0.28 mmol). After 1 h of stirring at room temperature, the solution was filtered off, and the solvent was evaporated to dryness. The white solid obtained was washed with hexane (2 × 20 mL) and then dried under vacuum: yield 0.3 g, 91%. Anal. Calcd for $C_{51}H_{45}AuClMnNO_7P_3$:

---

[10] Teo, B. K.; Hong, M. C.; Zhang, H.; Huang, D. B. *Angew. Chem., Int. Ed. Engl.* **1987**, *26*, 897.

[11] Carriedo, G. A.; Riera, V. *J. Organomet. Chem.* **1981**, *205*, 371.

[12] Prepared using the general procedure described for the syntheses of *fac*-$[Mn(L)(CO)_3(dppm)]ClO_4$ by: Carriedo, G. A.; Riera, V. *J. Organomet. Chem.* **1981**, *205*, 371.

[13] Braunstein, P.; Lehner, H.; Matt, D. *Inorg. Synth.* **1990**, *27*, 218.

[14] Teo, B.; Calabrese, J. C. *Inorg. Chem.* **1976**, *15*, 2467.

[15] Cotton, F. A.; Falvello, L. R.; Uson, R.; Fornies, J.; Thomas, M.; Casas, J. M.; Ara, I. *Inorg. Chem.* **1987**, *26*, 1366.

Table VI. Summary of Crystallographic Data

	compd **3a**	compd **6a**†
formula	$C_{51}H_{45}AgClMnNO_7P_3$	$C_{69}H_{59}AgAuClMn$-$NO_7P_6\cdot 0.5CH_2Cl_2$
cryst size, mm	0.40 × 0.40 × 0.40	0.17 × 0.13 × 0.13
cryst color	pale yellow	colorless
cryst syst	monoclinic	monoclinic
space group	$P2_1/c$	$P2_1/n$
Z	4	4
a, Å	11.828 (3)	14.192 (3)
b, Å	24.518 (5)	20.622 (6)
c, Å	17.293 (6)	24.37 (1)
β, deg	94.94 (3)	94.91 (3)
V, Å^3	4996 (2)	7106 (5)
$F(000)$	2192	3224
D_{exptl}, g cm^{-3}	1.43	1.51
μ(Mo Kα), cm^{-1}	8.27	27.45
diffractometer	Enraf-Nonius CAD4	Enraf-Nonius CAD4
monochromator	graphite	graphite
radiation: λ, Å	0.710 73	0.710 73
temp, °C	20	20
scan type	ω–2θ	ω–2θ
scan range	0–25	0–25
hkl range		
min	−14,0,0	−16,0,0
max	14,29,20	16,24,28
drift cors	0.98–1.00	0.98–1.40
abs cors		
ψ scans	0.98–1.00	0.92–1.00
DIFABS	0.78–1.23	0.67–1.23
no. of unique rflns	8718	12 399
R_{int} (some double measd)	0.022	0.056
no. of obsd rflns (criteria)	5822 ($I > 3\sigma$)	4830 ($I > 3\sigma$)
no. of variables	600	778
R	0.033	0.045
R_w	0.036	0.044
g	0.000 24	0.0003
residual electron density, e Å^{-3}	0.41 (−0.32)	1.32 (−0.70)
max shift/error	0.06	0.04 (0.5 for solvent)

C, 52.62; H, 3.90; N, 1.20. Found: C, 52.72; H, 4.00; N, 1.12.

Method b. To a solution of **3a** (0.10 g, 0.093 mmol) in CH_2Cl_2 (40 mL) was added 1 equiv (46 mg, 0.093 mmol) of $[AuCl(PPh_3)]$. The colorless solution was then stirred for 20 min, during which time a white precipitate of $[AgCl(PPh_3)]_4$ appeared. A 10-mL volume of hexane was then added, and the solution was filtered through a layer of Kieselgur (1 cm) to remove $[AgCl(PPh_3)]_4$. After concentration of the solution, hexane was added to obtained 80 mg of white crystalline solid (74% yield).

The complex $[Mn(CO)_4\{[Ph_2P)_2CH(AuPPh_3)\}]ClO_4$ (**4b**) was prepared by using method b, from **2b** (0.15 g, 0.147 mmol) and $[AuCl(PPh_3)]$ (73 mg, 0.147 mmol): yield 77%. Anal. Calcd for $C_{47}H_{36}AuClMnO_8P_3$: C, 50.90; H, 3.27. Found: C, 50.78; H, 3.29.

***fac*-[Mn(CNBu^t)(CO)$_3${(Ph$_2$P)$_2$C(AuPPh$_3$)$_2$}]ClO$_4$ (5a).** To a solution of *fac*-$[Mn(CNBu^t)(CO)_3(dppm)]ClO_4$ (**1a**; 0.20 g, 0.28 mmol) in 40 mL of CH_2Cl_2 were added KOH (0.40 g, 7.1 mmol) and $[AuCl(PPh_3)]$ (0.28 g, 0.567 mmol). The reaction was monitored by IR spectroscopy. After 20 min of stirring at room temperature the bands corresponding to **4a** were observed. An IR spectrum of the solution measured after 2 h showed only IR bands due to the complex **4a**. The solution was then filtered and concentrated to ca. 15 mL. The addition of hexane (30 mL) caused precipitation of a white solid (0.41 g, 89%). Anal. Calcd for $C_{69}H_{59}Au_2ClMnNO_7P_4$: C, 51.08; H, 3.66; N, 0.86. Found: C, 51.19; H, 3.72; N, 0.84.

The complex $[Mn(CO)_4\{(Ph_2P)_2C(AuPPh_3)_2\}]$ (**5b**) was obtained by following a similar procedure, with $[Mn(CO)_4(dppm)]ClO_4$ (**1b**; 0.10 g, 0.154 mmol), KOH (0.20 g, 3.56 mmol), and $[AuCl(PPh_3)]$ (0.153 g, 0.31 mmol): yield 0.21 g, 87%. Anal. Calcd for $C_{65}H_{50}Au_2ClMnO_8P_4$: C, 49.81; H, 3.22. Found: C, 49.86; H, 3.24.

[Mn(CNBu^t)(CO)$_3${(Ph$_2$P)$_2$C(AgPPh$_3$)(AuPPh$_3$)}]ClO$_4$ (6a). A solution of **4a** (0.108 g, 0.093 mmol) in CH_2Cl_2 (30 mL) was treated with $[AgCl(PPh_3)]_4$ (0.038 g, 0.0234 mmol) and an excess of KOH (0.20 g, 3.56 mmol). The mixture was stirred at room temperature for 2 h, and the completeness of the reaction was checked by IR spectroscopy; the reaction was stopped when only the ν(CO) pattern of **6a** was present. The solution was filtered off and concentrated under vacuum to about 10 mL, and then toluene (20 mL) was added. A 0.11 g amount of white crystals was obtained (77% yield). Anal. Calcd for $C_{69}H_{59}AgAuClMnNO_7P_4$: C, 54.05; H, 3.88; N, 0.91. Found: C, 54.17; H, 3.91; N, 0.89.

X-ray Structural Data for 3a and 6a†. Crystal data collection parameters for **3a** and **6a**† are summarized in Table VI. Single crystals of **3a** and **6a**† were grown by slow diffusion of liquid diethyl ether into a dichloromethane solution of the compound. Unit cell dimensions were determined from the angular settings of 25 reflections with $15° < \theta < 17°$ for **3a** and $9° < \theta < 16°$ for **6a**.† Intensity was checked throughout data collection by monitoring three standard reflections every 60 min. Final drift corrections are shown in Table VI. On all reflections, profile analysis was performed.[16,17] Some double-measured reflections were averaged; $R_{int} = \sum(|I| - \langle I \rangle)/\sum I$. Lorentz and polarization corrections were applied and data reduced to $|F_o|$ values. Semiempirical absorption corrections, ψ-scan based, were applied.[18]

Both structures were solved by Patterson interpretation using the program SHELXS86[19] and completed by the phase expansion procedure of DIRDIF.[20] Isotropic least-squares refinement, using SHELX76,[21,22] converged to $R = 0.083$ for **3a** and 0.077 for **6a**†. Additional empirical absorption correction was applied.[23] Further refinements included anisotropic thermal parameters for all non-hydrogen atoms. All hydrogen atoms were isotropically refined with a common thermal parameter riding on their parent atoms, except H(1), in molecule **3a**, for which coordinates and thermal parameters were refined. The function minimized was $\sum w(F_o - F_c)^2$, ($w = 1/(\sigma^2(F_o) + gF_o^2)$, with $\sigma(F_o)$ being obtained from counting statistics).

For structure **6a**†, one fairly disordered CH_2Cl_2 solvent molecule was found and refined with a half-occupancy factor. The Ag atomic site was partially substituted by Au atoms, resulting in a refined occupancy factor of 0.60 (1) in Ag.

Atomic scattering factors were taken from ref 24. The plots in Figures 1 and 2 were made with the PLUTO program.[25] Geometrical calculations were made with PARST.[26] All calculations were made on a MicroVax-3400 computer at the Scientific Computer Center, University of Oviedo.

Acknowledgment. We thank the Dirección General de Investigación Científica y Técnica (Spain) for financial support (Projet PB 88-0467) and for a research grant (to J.R.).

Supplementary Material Available: Complete listings of bond lengths and angles, anisotropic thermal parameters, hydrogen atom parameters, distances and angles involving H atoms, least-squares-planes data, and principal torsion angles for compounds **3a** and **6a**† (38 pages). Ordering information is given on any current masthead page.

OM920345T

---

(16) Lehman, M. S.; Larsen, F. K. *Acta Crystallogr.* **1974**, *A30*, 580.

(17) Grant, D. F.; Gabe, E. J. *J. Appl. Crystallogr.* **1978**, *11*, 114.

(18) North, A. C. T.; Phillips, D. C.; Mathews, F. S. *Acta Crystallogr.* **1968**, *A24*, 351.

(19) Sheldrick, G. M. SHELX86. In *Crystallographic Computing 3*; Sheldrick, G. M., Krüger, C., Goddard, R., Eds.; Clarendon Press: Oxford, England, 1985; pp 175–189.

(20) Beurskens, P. T.; Admiraal, G.; Behm, H.; Beurskens, G.; Bosman, W. P.; García-Granda, S.; Gould, R. O.; Smits, J. M. M.; Smykalla, C. *Z. Kristallogr.* **1991**, *4*, 99.

(21) Sheldrick, G. M. SHELX, A Program for Crystal Structure Determination; University Chemical Laboratory: Cambridge, England, 1976.

(22) Van der Maelen, J. F. Ph.D. Thesis, University of Oviedo, Oviedo, Spain, 1991.

(23) Walker, N.; Stuart, D. *Acta Crystallogr.* **1983**, *A39*, 158.

(24) *International Tables for X-Ray Crystallography*; Kynoch Press: Birmingham, England, 1974; Vol. IV.

(25) Motherwell, W. D. S.; Clegg, W. PLUTO, A Program for Plotting Molecular and Crystal Structures; University Chemical Laboratory: Cambridge, England, 1978.

(26) Nardelli, M. *Comput. Chem.* **1983**, *7*, 95.